

# ANFIS-Fuzzy Logic-based Hybrid DFIG and PMSG Grid Connected System with TCSC

K.KARTHI, A. RAMKUMAR

Dept of EEE., Kalasalingam Academy of Research and Education (KARE), Srivilliputhu,  
Tamilnadu, INDIA

**Abstract:** Variable-speed wind turbines might provide green electricity. Grid operators' grid regulations require wind turbines to recover from grid disruptions and help maintain electricity networks. Having wind turbines equipped with fault current limiters (FCLs) may ensure their continued functioning in the event of a power loss. In this piece, we will talk about how to improve the two most common types of variable-speed wind turbines: the Doubly Fed Induction Generator (DFIG) and the Permanent Magnet Synchronous Generator (PMSG). Both wind generators were evaluated using the Thyristor Controlled Series Compensator (TCSC) with ANFIS and Fuzzy Logic. It is important to understand the dynamic behavior of wind turbines, hence models of their FCLs were built for steady state and grid disruptions. Power interruptions switched the FCLs in both wind turbines utilising grid voltage variation. Both wind turbines underwent a no-control FCL scenario. Both wind turbines' FCLs were measured and compared under load from a severe three-phase to ground failure at their terminals. Both wind turbines were operated under similar circumstances to examine FCL control tactics during power interruptions.

*Keywords:* ANFIS, Fuzzy Logic, Total Harmonic Distortions, Wind Energy conversion system, DFIG, and PMSG Control.

Received: February 23, 2023. Revised: November 15, 2023. Accepted: December 15, 2023. Published: January 30, 2024.

## 1. Introduction

It is crucial to acquire new methods of power grid stabilization for smooth operation [1,2] since wind energy penetration into existing power grids develops day by day, with an average projection of 75 GW per year during the 2021-2026 timeframe. Wind farms are an emerging industry that requires sophisticated voltage and frequency control to meet their grid requirements. As a result of the broad operating window afforded by variable-speed wind turbine technology [3], these machines are more common. The two most common types of variable-speed wind turbines used in current wind farms are the DFIG and the PMSG.

The development of power electronics and drives in control mechanisms has greatly facilitated the transition of wind turbines from fixed speed to variable speed technology [4,5]. Advantages of fixed-speed wind turbines include their simplicity, durability, affordability, and minimal maintenance requirements. However, there are significant challenges associated with this type of wind turbine, which prevent it from being widely used in wind energy applications. These include a lack of control over voltage and frequency and the need for substantial reactive power during grid

disturbances to survive air-gap flux recovery. Thus, variable-speed wind turbines are employed in the building of contemporary wind farms because of their high energy capture efficiency, effective voltage management, and lower mechanical drive train stress [6]. Both the DFIG and PMSG wind turbine technologies use a series connections of power converters. The PMSG's high initial cost is owing to its full-rated power converters, whereas the DFIG's gearbox system has a lower power converter rating of 20-30 percent. Active and reactive power management is simplified by the DFIG technology's architecture, which links the Rotor Side Converter (RSC), also known as the Machine Side Converter (MSC), and the Stator Side Converter (SSC), also known as the Grid Side Converter (GSC), through the DC-link voltage.

These wind turbines have a great pitch adjustment system that allows them to recover their voltage after grid disturbances [9,10] and operate in a broad range to maximize energy absorption [7,8]. However, the back-to-back power converter in a PMSG wind turbine is fully rated, whereas that in a DFIG wind turbine is only rated at 50%. This kind of wind turbine is thus more likely to provide optimal adaptability

and superior control over active and reactive power. However, the PMSG's prohibitive upfront cost is a major drawback. Numerous control schemes, such as FCLs in DFIG wind turbines [11–14], reactive power compensation, crowbar, and DC chopper [15–16], and sliding mode control for Maximum Power Point Tracking (MPPT) [17–18], have previously been reported in the literature. Methods for wind energy conversion were provided in [22] and the Fault Ride Through (FRT) assessment of a DFIG wind turbine was conducted using several control topologies in [19–21].

However, in [23,24], the DC-link voltage was maintained at its limit during a grid failure, and the maximum current and MPPT power converters for the PMSG wind turbine were investigated. [25] bolstered the performance of the PMSG turbine with the aid of a superconducting fault current limiter (SFCL) control mechanism. This study investigated the permanency problems of DFIG and PMSG wind turbines and how their augmentation evaluations compare to existing FCLs. Similar studies can be found in [26–28]. Both types of wind generators' control topologies and wind turbine-modeling elements were detailed. Both wind turbines had a severe bolted three-line-to-ground failure with no FCL control or augmentation strategy to test the controllers' robustness. The mathematical dynamics of inserting SDBR, BFCL, and CBFCL at the stator of both wind turbines under similar operating circumstances were also supplied for fair comparison. Each wind turbine system used an SDBR with the same effective size and the same BFCL and CBFCL parameters. During a grid failure, the grid voltage was utilized as the switching signal. Only a small number of articles in the scholarly literature investigate the presence of these FCLs in both types of wind turbines. FRT enhancement of both wind turbines has only been briefly touched on in a few of the aforementioned papers.

## 2. The System Model

### 2.1 Modelling of DFIG

To simplify, the DFIG may be seen as a conventional induction generator with a nonzero

rotor [8]. Both the rotor converter, which regulates the rotational speed of the generator, and the grid converter, which injects reactive energy into the grid, make up the power converter of a wind turbine. The actual and reactive power components of the grid-side converter (GSC) are shown in Figure 1. According to [9], in a synchronously rotating direct-quadrature (d-q) reference frame, the dynamic equation of a three-phase DFIG's voltages and flux connections may be written as (1) through (8):

### 2.2. DFIG Control Model

and reactive power is regulated by the RSC controller, while DC-link voltage and reactive power injection into the grid are managed by the grid-side converter (GSC) controller. In a Graetz bridge configuration, snubber resistance and capacitance are added to the RS of a three-phase IGBT-diode rectifier to dampen vibrations. The DC bus capacitor voltage is controlled by the grid-side converter [11]. By adjusting the pitch angle, we can determine how much energy can be harvested in strong winds. A torque controller is used in the control system to maintain a consistent velocity. The reactive power of the wind turbine is likewise kept at 0 MVAR. The control equations, as seen from the rotor, might be represented in the form of Figure 2.

### 2.3 Grid Side Controller

Maintaining a fixed DC-link voltage regardless of the magnitude or direction of the rotor's power flow [12] is the primary goal of the GSC. To accomplish this, we use the hysteresis current control approach shown in Figure 2, which uses a reference frame that is co-linear with the stator voltage position. The reactive power and the DC-link voltage between the converter and the grid may thus be independently controlled.

In a voltage vector-oriented reference frame, the current regulates the DC-link voltage. Therefore, as illustrated in Figure 2, a reference current value is calculated by tuning a PI controller using the DC-link voltage error  $e$  and the error variation.

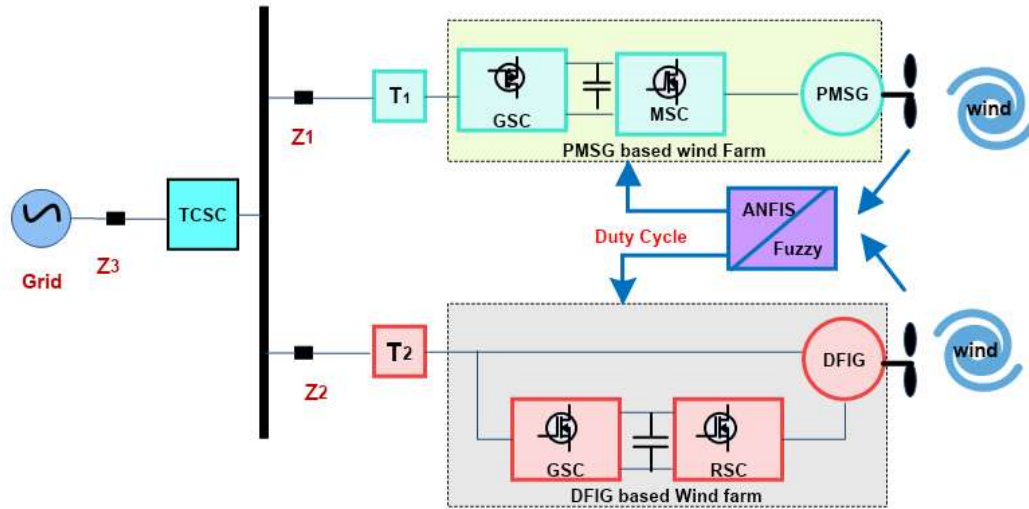


Fig. 1: General block diagram of the proposed system

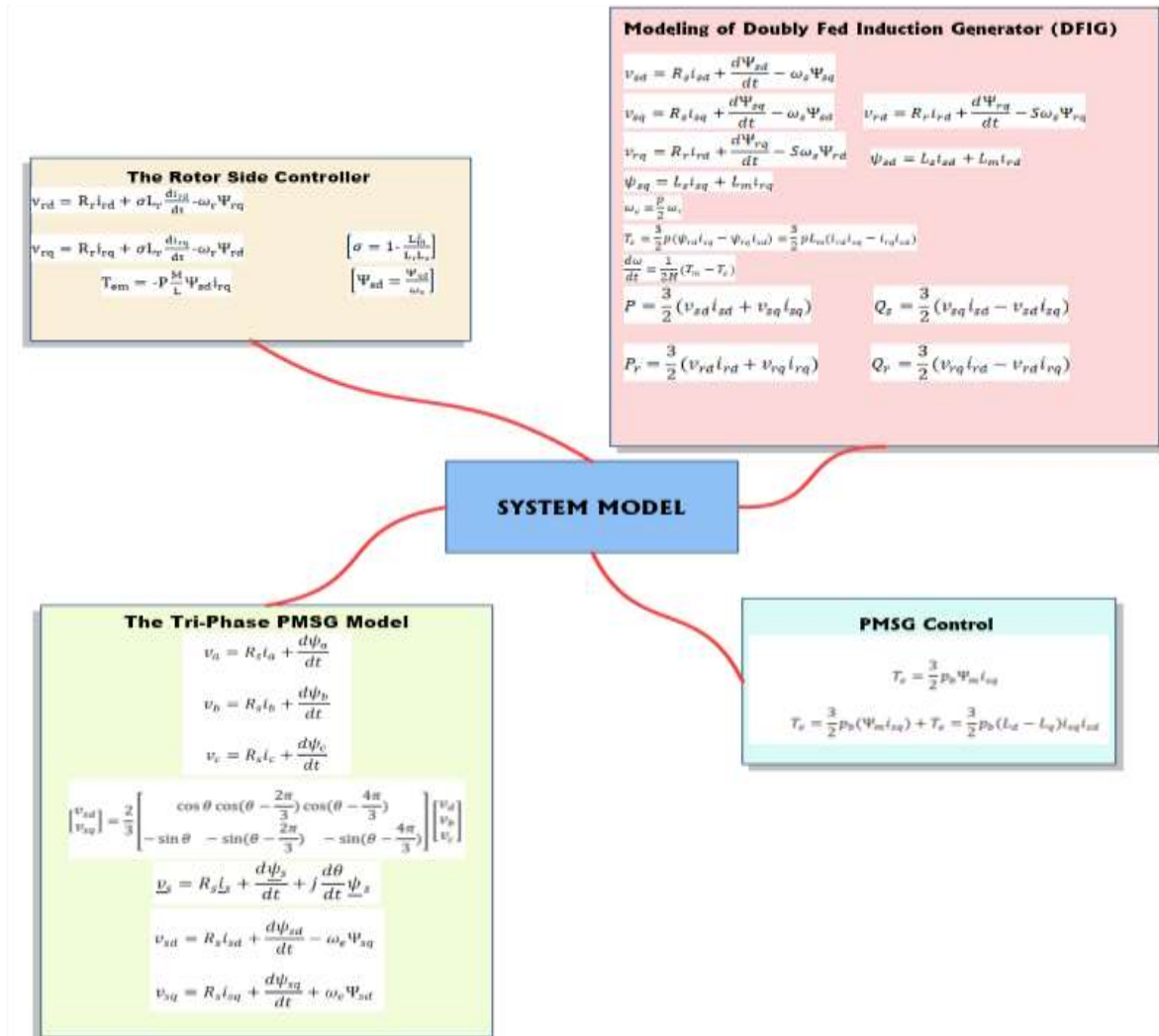


Fig. 2: Mathematical modeling of Hybrid system

### 3. Thyristor Controlled Series Compensator

The benefits of series capacitors over shunt capacitors are substantial. The reactive power of a series capacitor is proportional to the square of the line current, whereas the reactive power of an inductor-capacitor is related to the square of the short circuit in a bus circuit. The reactive power rating of a shunt capacitor typically has to be three to six times higher than that of a series capacitor to provide the same system advantages as those of a series capacitor. Additionally, shunt capacitors often need to be linked in the middle, while series capacitors have no such need.

#### 3.1 Operation of TCSC controller.

Continuous control of power on the AC line is made possible by a TCSC, a series-regulated capacitive reactance. Analyzing the operation of a TCSC may be reduced to a few simple steps by considering the effects of a variable induction linked in series with a constant capacitor, as seen in Fig. 3. This combination's equivalent impedance,  $Z_{eq}$ , may be written as

$$Z_{eq} = \left( j \frac{1}{\omega C} \right) || (j\omega L) = -j \frac{1}{\omega C - \frac{1}{\omega L}} \quad (1)$$

If  $\omega C - \left( \frac{1}{\omega L} \right) > 0$  or  $\omega L > \left( \frac{1}{\omega C} \right)$ , Since the FC's reactance is below the along a variable reactor's, the resulting reactance is adjustable capacitance. If  $\omega C - \left( \frac{1}{\omega L} \right) = 0$ , Inadequate conditions include the development of a resonance leading to infinite capacitive impedance. If  $\omega C - \left( \frac{1}{\omega L} \right) < 0$ , Therefore the inductance provided by the combination is greater than that of a fixed inductor. In this case, the TCSC is operating in its inductive micrometre mode.

Analysis of a TCSC behaves similarly to that of an LC parallel combination when the voltage and current in the circuit are pure sinusoids. In contrast, thyristor switching causes non-sinusoidal voltage and current in a TCSC's fuel cell (FC) and thyristor-controlled reactor (TCR). Further sections elaborate on how TCSC operates in detail.

The DFIG and PMSG generator data tables 1 and 2 each include information for one turbine used in simulations.

**TABLE 1:** The Design Parameters Of DFIG

Generator Data for one Turbine	
Nominal Electrical Power	1.5MVA
Stator Resistance, $R_s$	0.23p.u.
Rotor Resistance, $R_r$	0.016 p.u.
Stator Inductance, $L_s$	0.18 p.u.
Rotor Inductance, $L_r$	0.16 p.u.
Magnetizing inductance, $L_m$	2.9 p.u.
Inertia Constant, H	0.685
Pole Pair, p	3

**TABLE 2:** The Design Parameters Of PMSG

Generator Data for one Turbine	
Nominal Electrical Power	1.5MVA
GS coupling impedance	0.00 p.u.
D.C. Capacitor (V)	1150
Number of pole pairs	48
Feedback time Constant (s)	2.9 p.u.
Inertia Constant, H	0.005
Pole Pair, p	3

### 4. Discussion of the Findings

The PMSG rating system is identical to the DFIG rating system. Figure 4 depicts the Simulink equivalent circuit diagram for this system. To assess the performance of Hybrid PMSG and DFIG in terms of output powers (P&Q), voltages and current, THD, and dynamic responses with ANFIS and with Fuzzy based TCSC, a failure (time = 1 Sec to 1.75 Sec) is simulated for both machine side bus (B575). The active and reactive powers are given in Figs. 5, 6, and 7, respectively, for comparison. The oscillations in DFIG+PMSG with ANFIS-based TCSC active power are demonstrated in Figure 10 to be substantially lower than those in DFIG+PMSG with Fuzzy based TCSC during fault. DFIG and PMSG with ANFIS based TCSC attain steady-state values after 3.5 seconds, however, with Fuzzy based TCSC, they continue to fluctuate even after 5 seconds. In addition, Figure 11 depicts the reaction of DFIG and PMSG reactive power with ANFIS based and with Fuzzy based TCSC. Reactive power regulation with ANFIS based TCSC at zero

MVAR is much superior than that with Fuzzy based TCSC during a malfunction. During a fault, the reactive power deviation from zero MVAR is substantially lower with ANFIS based TCSC than with Fuzzy based TCSC, but once the fault is cleared, the reactive power of with Fuzzy based TCSC recovers to zero in a much shorter time than with ANFIS based TCSC. As a result, if a system requires that reactive power be controlled at zero MVAR for an extended period and abrupt large deviations are permitted, then a system with Fuzzy based TCSC may be a preferable solution. Still, if a system requires that reactive power not move too much from zero MVAR, TCSC may be a preferable alternative. Figure 8 shows a voltage comparison with ANFIS based and with Fuzzy based TCSC. During the fault, the voltage of DFIG and PMSG with ANFIS based TCSC oscillates roughly 10% more than the voltage of DFIG and PMSG with Fuzzy based TCSC owing to flux oscillations necessary to supply the reactive power. This is because speed is inversely related to flux. Furthermore, DFIG and PMSG with ANFIS based TCSC have greater inertia due to their heavier weight than DFIG and PMSG with Fuzzy based TCSC. The voltage and current of DFIG and PMSG with

ANFIS based TCSC achieve steady-state in a much shorter time than DFIG and PMSG with Fuzzy based TCSC. DFIG and PMSG with ANFIS based TCSC achieve a steady-state value at  $t = 2.5$  seconds, but DFIG and PMSG with Fuzzy based TCSC fluctuate even at  $t = 4.5$  seconds. As a result, if the voltage and current control are more important, DFIG and PMSG with ANFIS based TCSC should be utilized; otherwise, DFIG and PMSG with Fuzzy based TCSC might be employed. THDs of voltages of DFIG and PMSG with Fuzzy based TCSC and DFIG and PMSG with ANFIS based TCSC are shown in Figs. 8 and 9, respectively, owing to fault. They demonstrate that harmonic distortion is lower in DFIG and PMSG with ANFIS based TCSC than in DFIG and PMSG with Fuzzy based TCSC; hence, power quality is optimum when DFIG and PMSG with ANFIS based TCSC are used with ANFIS based an innovative power electronic interface. As a result, it is determined that DFIG and PMSG with ANFIS based TCSC are more effective as wind turbine generators than DFIG and PMSG with Fuzzy based TCSC, and that unconventional power electronic interfaces are more effective as interfaces than standard power electronic interfaces

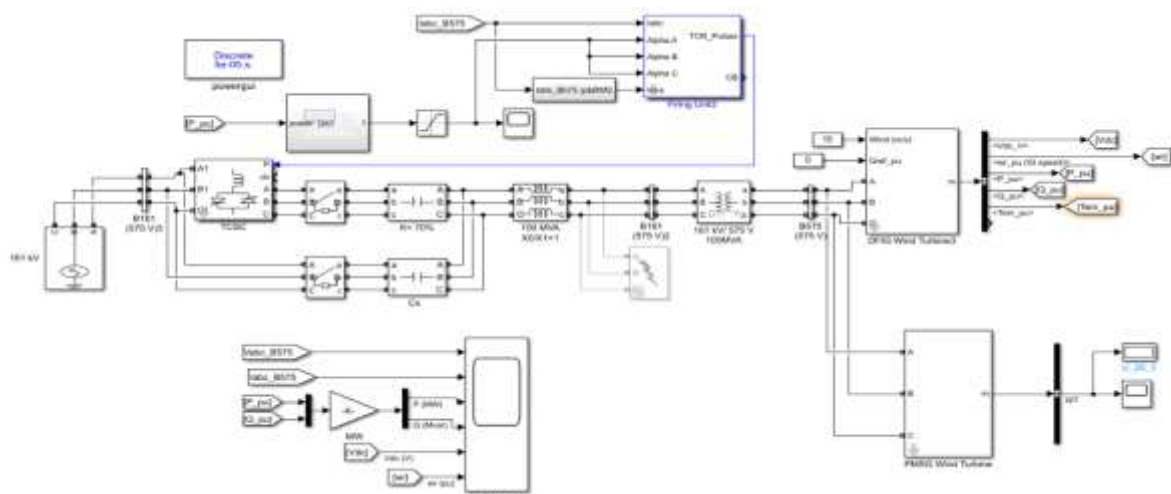


Fig. 3: The Simulink equivalent circuit diagram of DFIG and PMSG with ANFIS based TCSC system

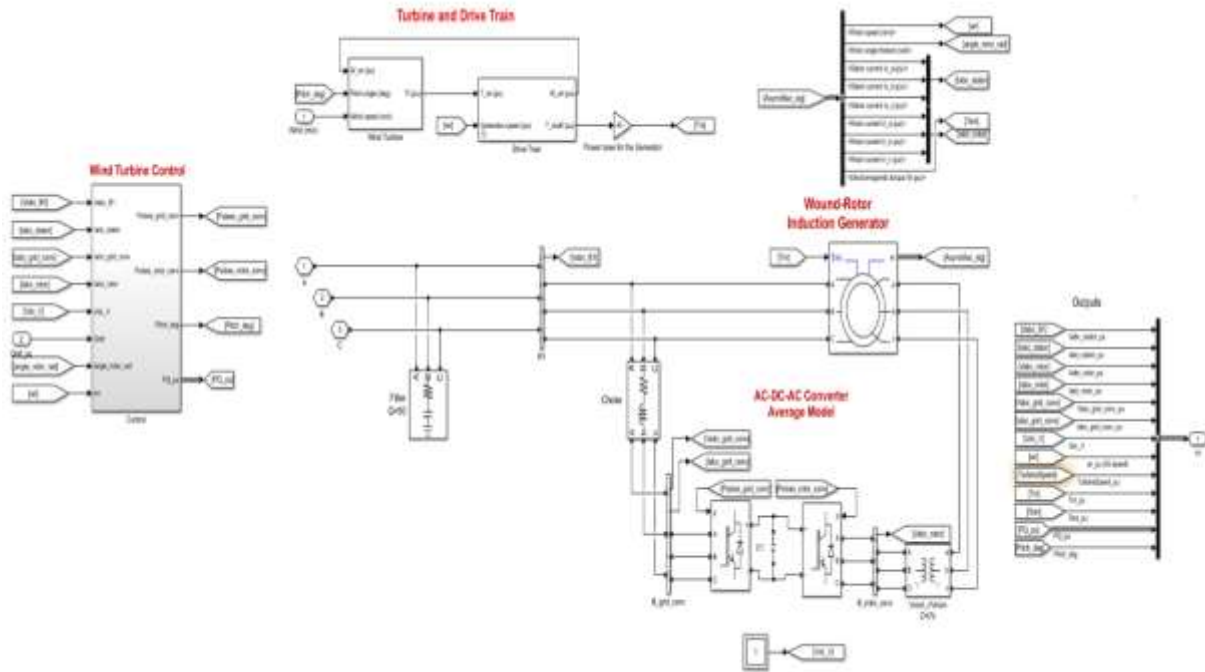


Fig. 4: Simulink diagram of DFIG system

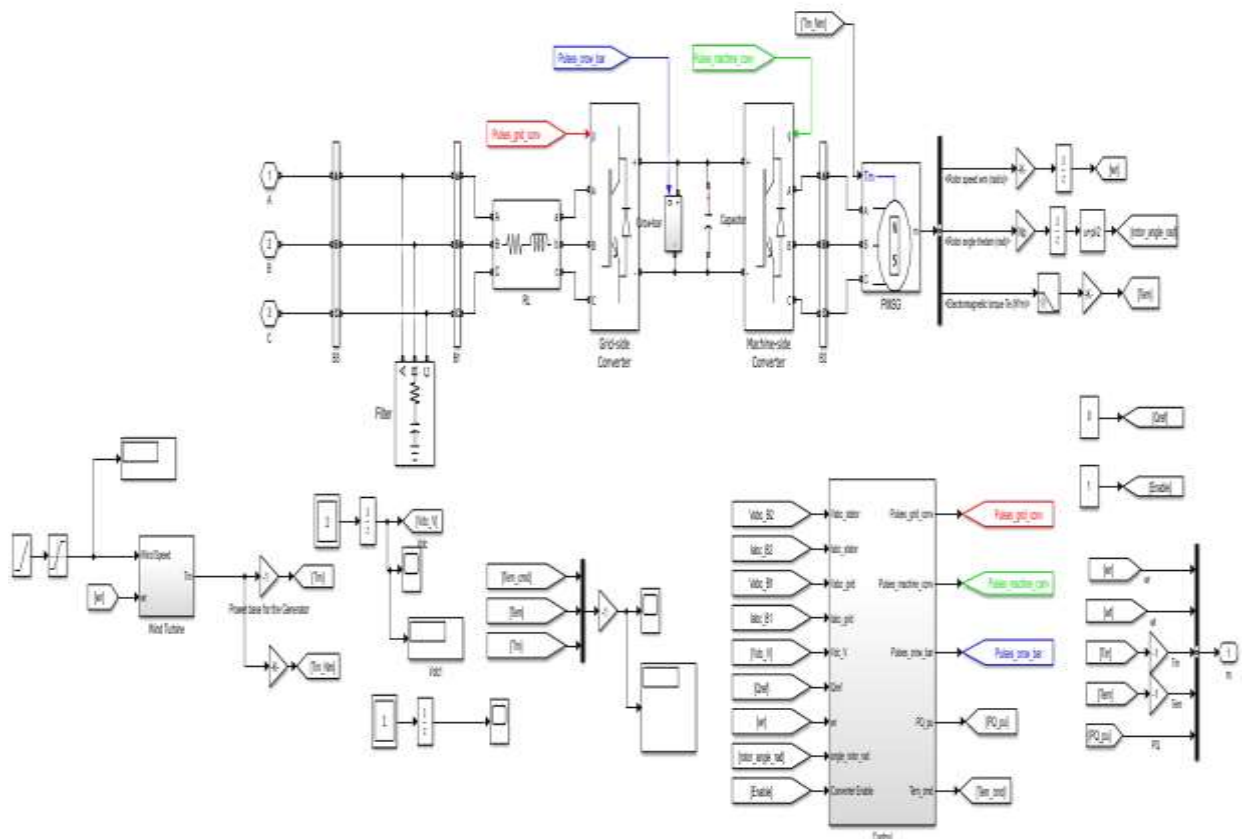


Fig. 5: Simulink diagram of PMSG with machine side and grid side controller

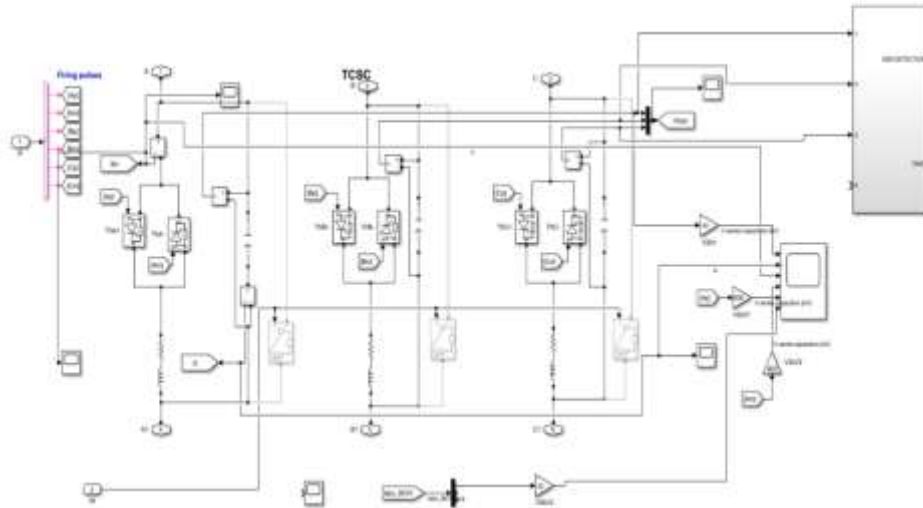


Fig. 6: Simulink diagram of TCSC controller

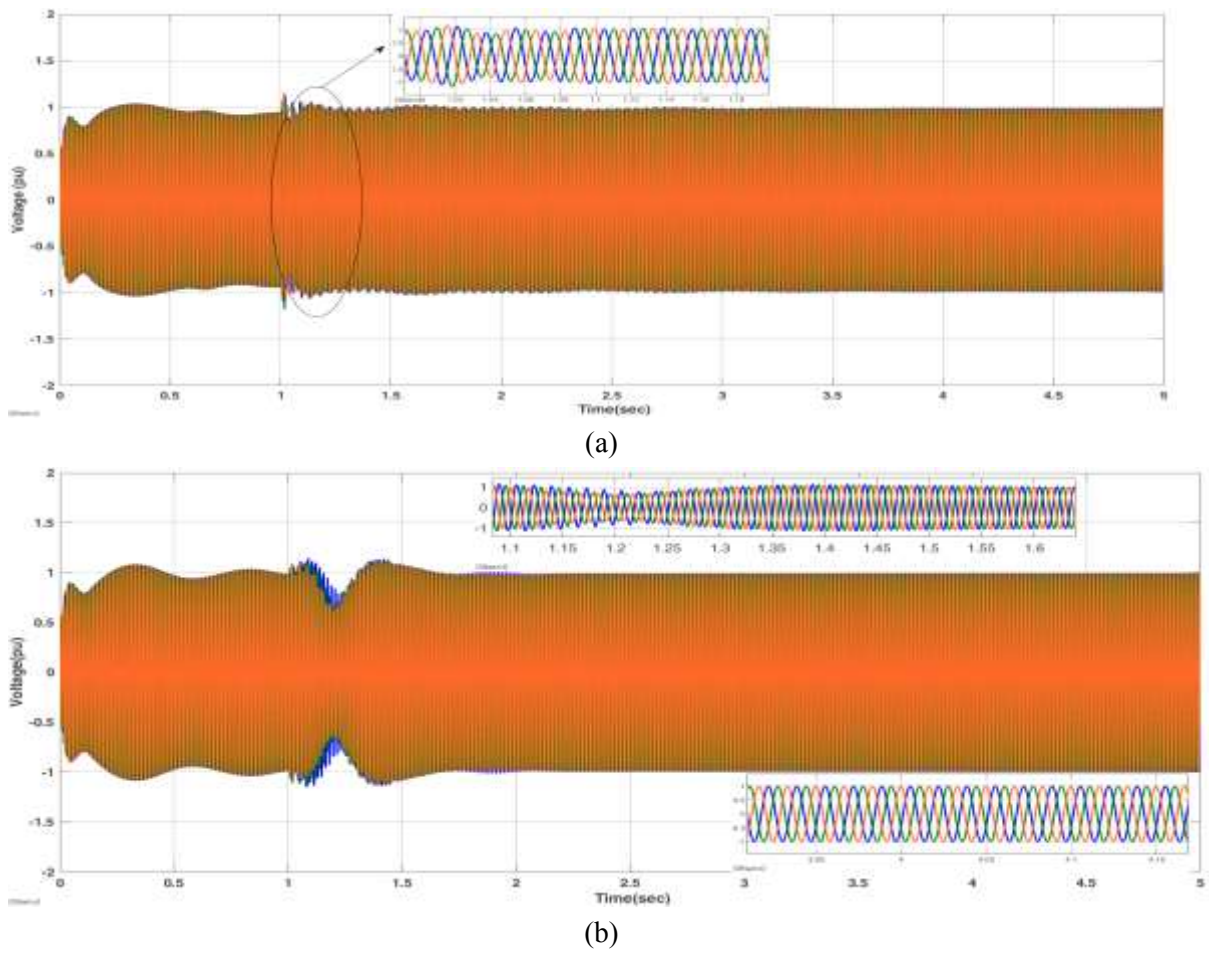
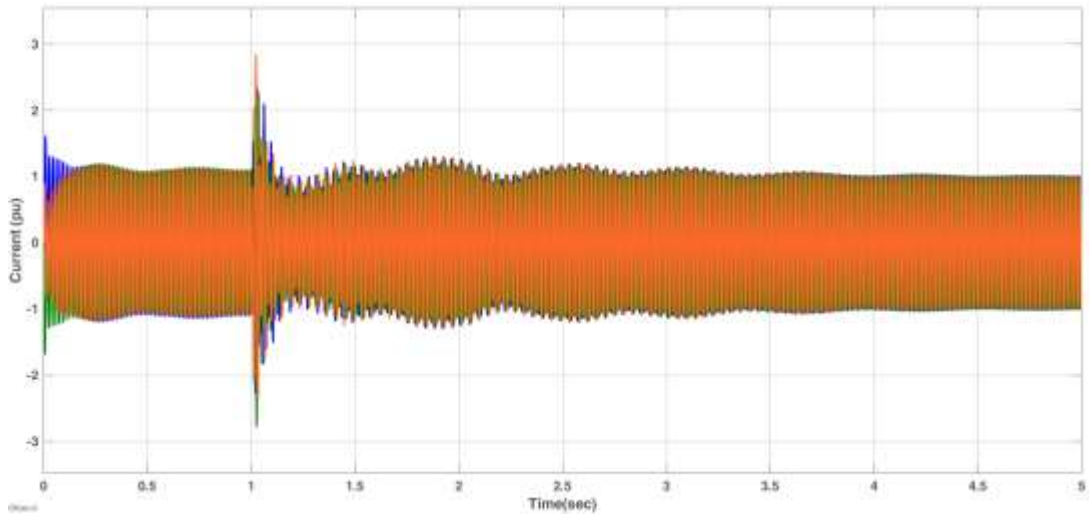
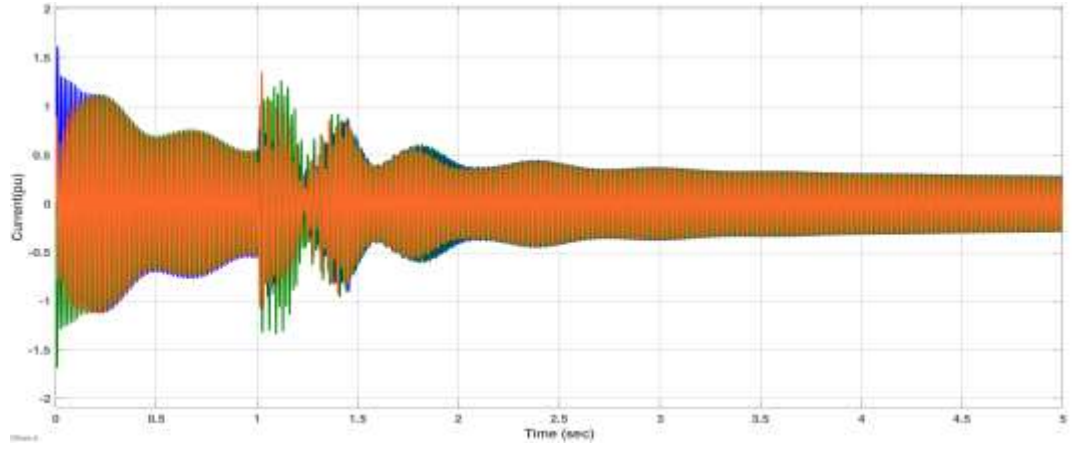


Fig. 7: Grid Side Output Voltage Fault created from 1 Sec to 1.75 Sec (a) DFIG and PMSG with Fuzzy based TCSC (b) DFIG and PMSG with ANFIS based TCSC

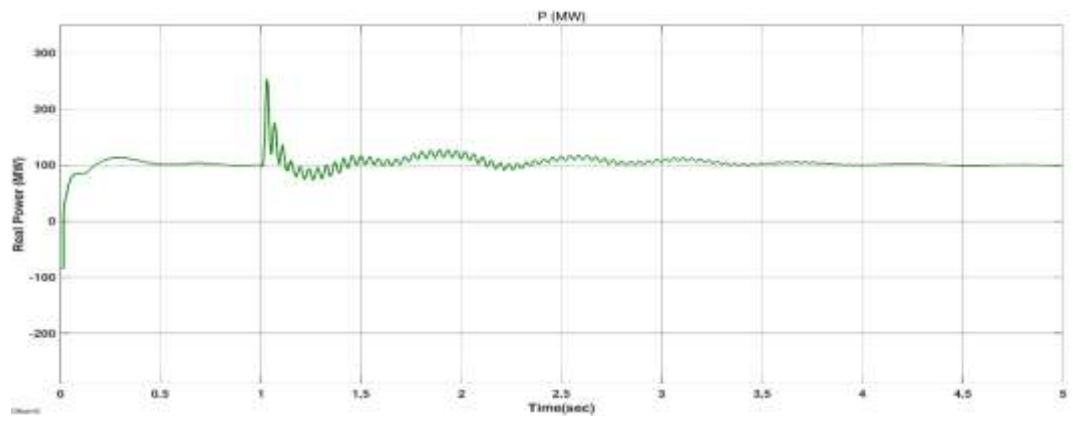


(a)



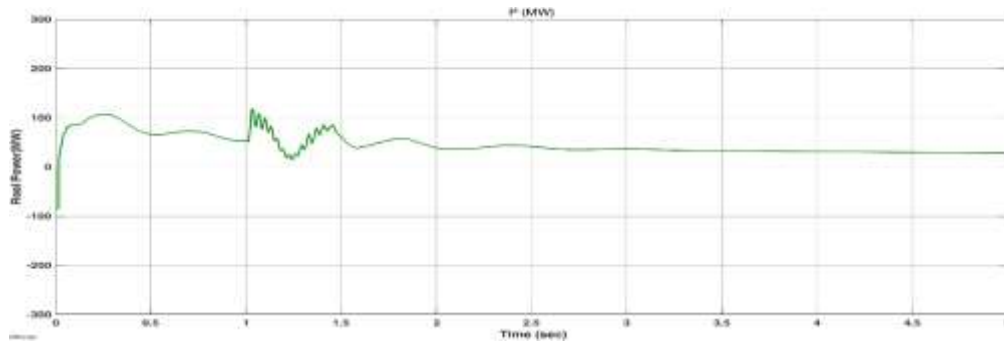
(b)

Fig. 8: Grid Side Output Current during the fault condition (Fault created from 1 Sec to 1.75 Sec) (a) with ANFIS based TCSC (b) with ANFIS based Fuzzy based TCSC



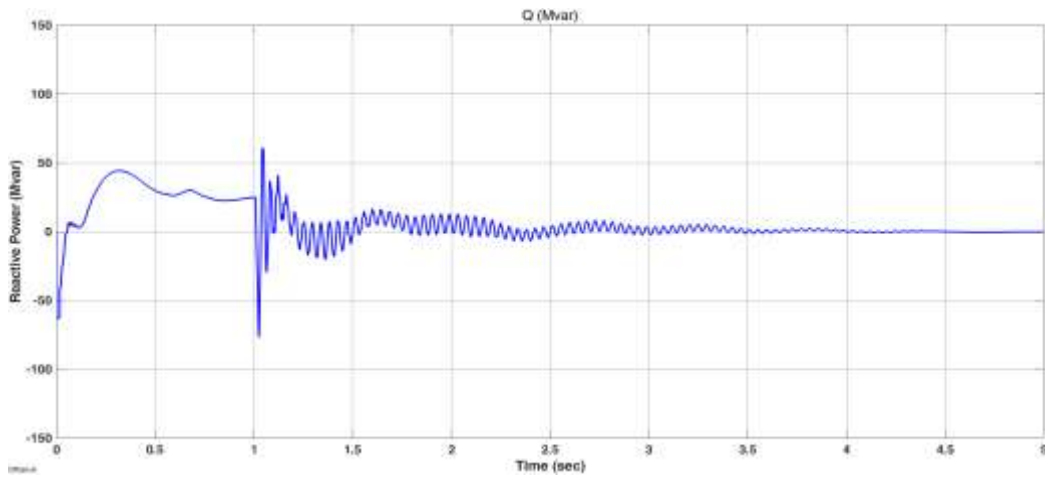
(a)





(b)

Fig. 9: Real power during the fault condition (Fault created from 1 Sec to 1.75 Sec) (a)with ANFIS based TCSC (b) with Fuzzy based TCSC



(a)

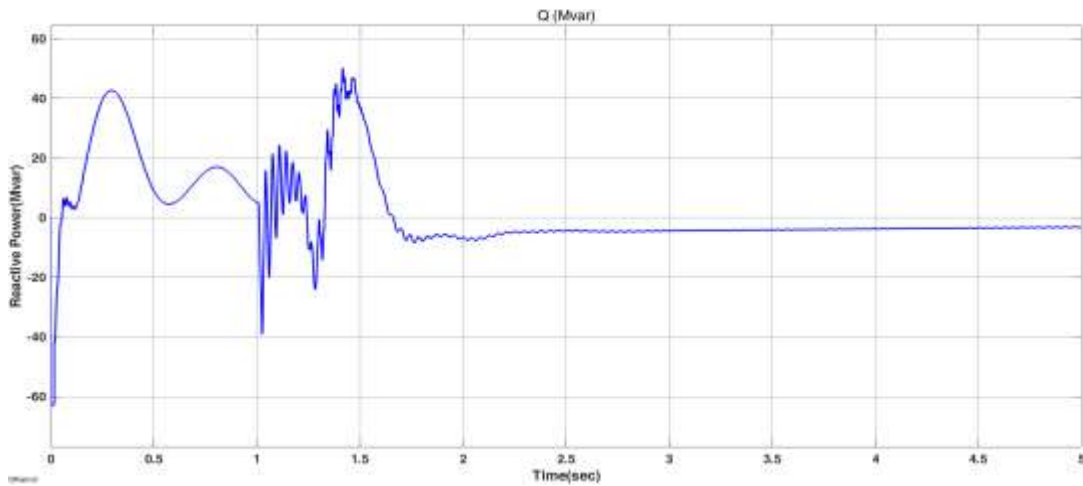


Fig. 10: Reactive power during the fault condition (Fault created from 1 Sec to 1.75 Sec) (a) with ANFIS based TCSC (b) with Fuzzy based TCSC

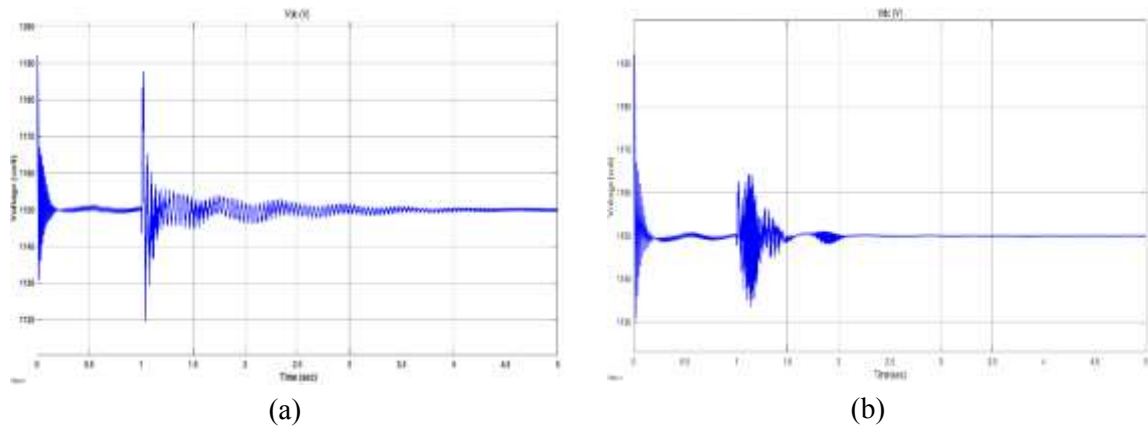


Fig. 11: DC link voltage with ANFIS based TCSC (b) with Fuzzy based TCSC

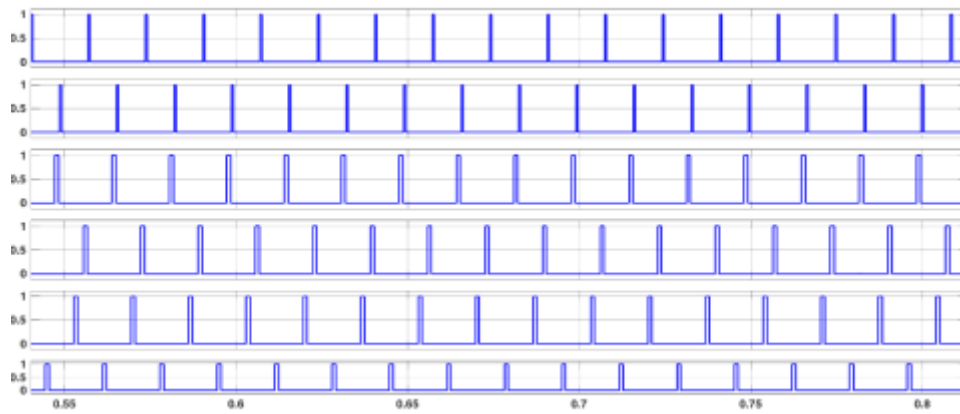


Fig. 12: Gate pulse

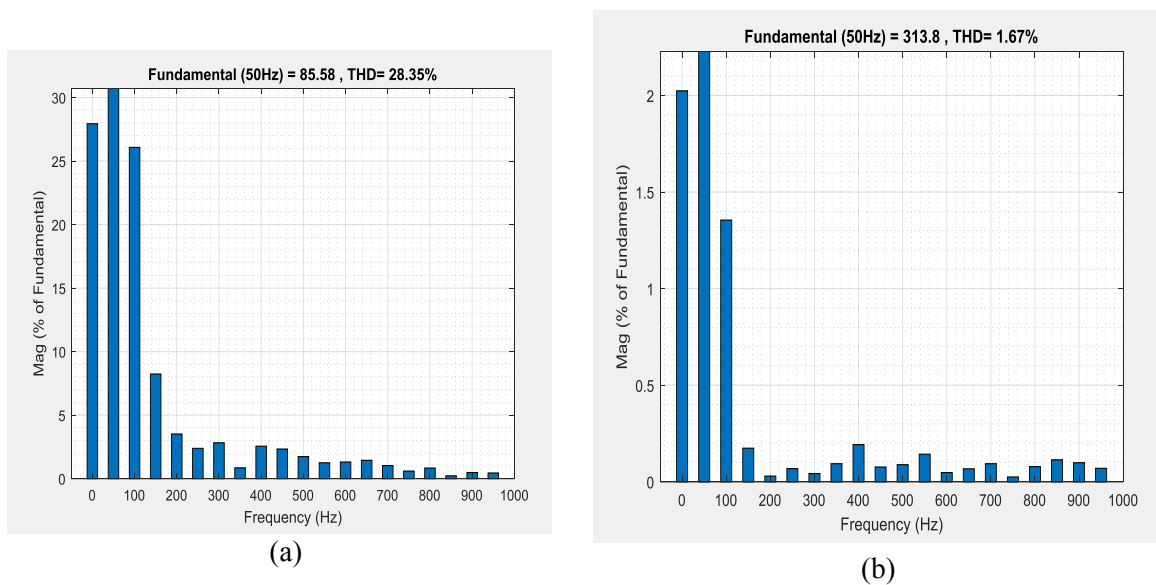


Fig. 13: THD Values (a) with Fuzzy based TCSC (b) with ANFIS based TCSC

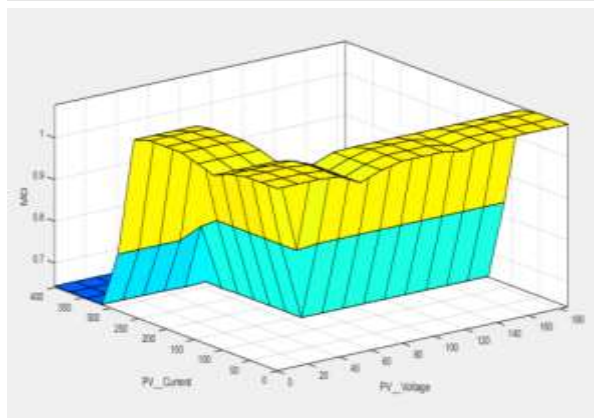
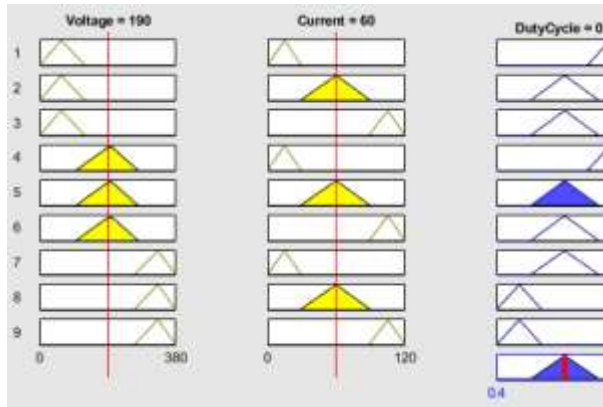
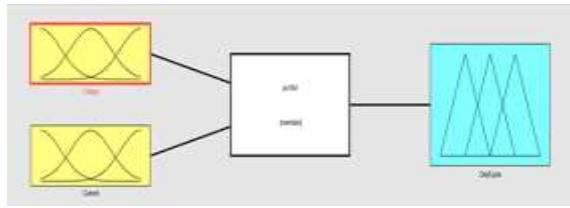
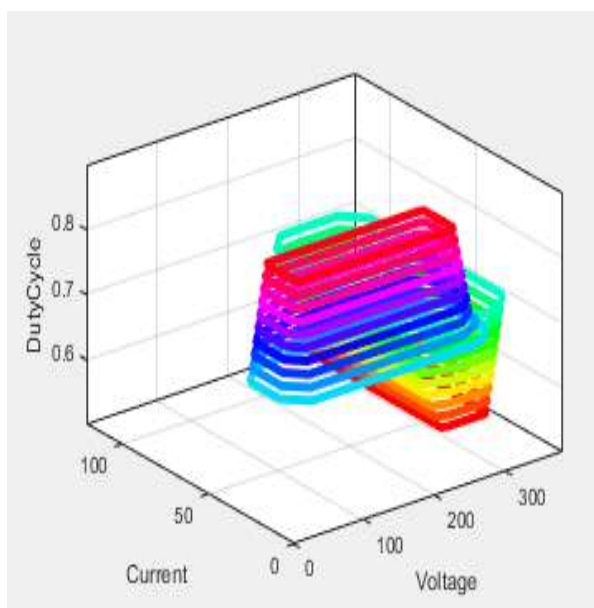
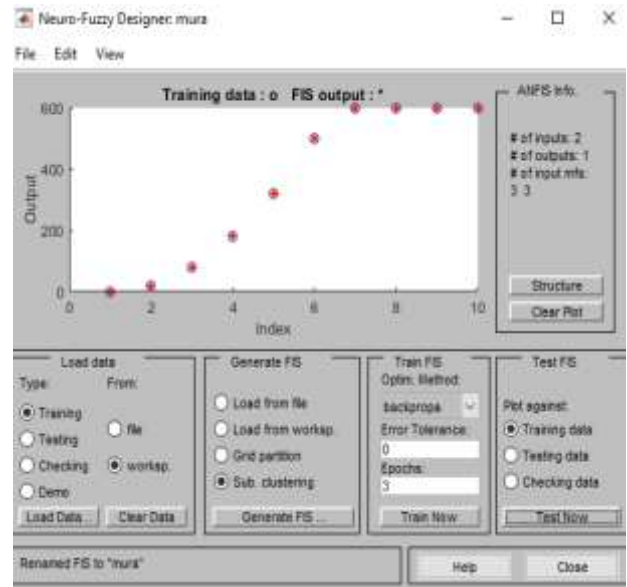


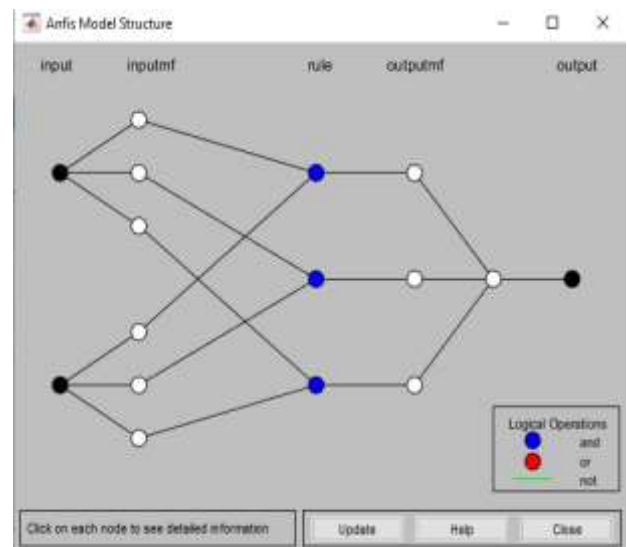
Fig. 14: Fuzzy logic rule viewers



(a)



(b)



(c)

Fig. 15: ANFIS based output (a) Surface Window (b) ANFIS Designer Window (c) ANFIS Structure Window

## 5. Conclusion

As a consequence, DFIG and PMSG with ANFIS based TCSC are more effective wind turbine generators than those with FUZZY based, and unconventional power electronic interface is more effective than standard power electronic interface. The comparison may be summed up by noting that during a fault, DFIG and PMSG with FUZZY based TCSC both use more reactive power than DFIG and PMSG with ANFIS based TCSC consume under the same circumstances, even after the improvement. The modifications

made to the DFIG and PMSG with Fuzzy based TCSC control assist in the oscillation reduction part of the machine's dynamic behavior. It takes far longer for DFIG and PMSG with Fuzzy based TCSC to recover their permanence than it does for DFIG and PMSG with ANFIS based TCSC, which implies that DFIG and PMSG with ANFIS based TCSC are more dependable than DFIG. On the other hand, the performance of the DFIG and PMSG with ANFIS based TCSC wind turbine was improved utilizing the TCSC with 9% overshoot and 2.35 s settling time for the actual and reactive power. The THD values were with ANFIS based TCSC at 1.67% with Fuzzy based TCSC at 28.35%. Moreover, a quicker settling time was also seen employing the TCSC for DFIG and PMSG. Except for the terminal grid voltage variable, the ANFIS based TCSC improved the performance of the DFIG and PMSG. To achieve optimal fault ride-through performance for a given application, it is advised to couple TCSC-based variable speed wind turbines with the DFIG and PMSG.

### References

- [1] Wind-Fuels and Technologies, International Energy Agency. 2021. Available online: <https://www.iea.org>.
- [2] Nduwamungu, A. Ntagwirumugara, E. Mulolani, F. Bashir, W., " Fault Ride through Capability Analysis (FRT) in Wind Power Plants with Doubly Fed Induction Generators for Smart Grid Technologies," *Energies* vol. 13, pp. 42-60,2020.
- [3] Sitharthan, R. Karthikeyan, M. Sundar, D.S. Rajasekaran, S. , "Adaptive hybrid intelligent MPPT controller to approximate effectual wind speed and optimal rotor speed of variable speed wind turbine," *ISA Transaction*, vol. 96, pp. 479–489,2020.
- [4] Okedu, K.E. Muyeen, S.M. Takahashi, R. Tamura, J., " Protection schemes for DFIG considering rotor current and DC-link voltage," In Proceedings of the 24th IEEE-ICEMS International Conference on Electrical Machines and System, Beijing, China, pp. 1–6, 20–23 August 2011.
- [5] Ouyang, J. Tang, T. Yao, J. Li, M., "Active Voltage Control for DFIG-Based Wind Farm Integrated Power System by Coordinating Active and Reactive Powers under Wind Speed Variations," *IEEE Transaction Energy Convers*, vol. 34, pp. 1504–1511,2019.
- [6] Okedu, K.E., " Introductory Chapter of the book Power System Permanency," INTECH: Horwich, UK, pp. 1–10,2019.
- [7] Shao, H. Li, Z. Zhou, D. Sun, S. Guo, L. Rao, F., "Permanency Enhancement and Direct Speed Control of DFIG Inertia Emulation Control Strategy," *IEEE Access*, vol. 7, pp. 120089–120105,2019.
- [8] He, X. Fang, X. Yu, J., " Distributed Energy Management Strategy for Reaching Cost-Driven Optimal Operation Integrated with Wind Forecasting in Multimicro grids System," *IEEE Transaction System Man Cyber. System*, vol.49, pp. 1643–1651,2019.
- [9] Qazi, H.W. Wall, P. Escudero, M.V. Carville, C. Cunniffe, N. Sullivan, J.O., "Impacts of Fault Ride Through Behavior of Wind Farms on a Low Inertia System," *IEEE Transaction Power System*, vol. 28, no. 1, 2020.
- [10] Chunli, L. Zefu, T. Huang, Q. Nie, W. Yao, J., "Lifetime Evaluation of IGBT Module in DFIG Considering Wind Turbulence and Nonlinear Damage Accumulation Effect," In Proceedings of the 2019 IEEE 2nd International Conference on Automation, Electronics and Electrical Engineering (AUTEEE), Shenyang, China, pp. 22–24, November 2019.
- [11] Okedu, K.E. Muyeen, S.M. Takahashi, R. Tamura, J., " Use of Supplementary Rotor Current Control in DFIG to Augment Fault Ride Through of Wind Farm as per Grid Requirement," In Proceedings of the 37th Annual Conference of IEEE Industrial Electronics Society (IECON 2011), Melbourne, Australia, pp.7–10, November 2011.
- [12] Okedu, K.E. Muyeen, S.M. Takahashi, R. Tamura, J., " Improvement of Fault Ride Through Capability of Wind Farm using DFIG Considering SDBR," In Proceedings of the14th European Conference of Power Electronics EPE, Birmingham, UK, pp. 1–10,2011.
- [13] Okedu, K.E., "Enhancing DFIG Wind Turbine during Three-phase Fault Using Parallel Interleaved Converters and Dynamic Resistor," *IET Renewable Power Generation*, vol. 10, pp. 1211–1219,2016.
- [14] Okedu, K.E. Muyeen, S.M. Takahashi, R. Tamura, J., " Participation of FACTS in Stabilizing DFIG with Crowbar during Grid Fault Based on Grid Codes," In Proceedings of the 6th IEEE-GCC Conference and Exhibition, Dubai, UAE, pp. 365–368, 2011.
- [15] Boujoudi, B. Kheddioui, E. Machkour, N. Achalhi, A. Bezza, M., " Comparative study between different types of control of the wind turbine in case of voltage dips," In Proceedings of

- the 2018 Renewable Energies, Power Systems & Green Inclusive Economy (REPS-GIE), Casablanca, Morocco, pp. 1–5, 2018.
- [16] Okedu, K.E. Muyeen, S.M. Takahashi, R. Tamura, J., "Comparative Study between Two Protection Schemes for DFIG-based Wind Generator," In Proceedings of the 23rd IEEE-ICEMS (International Conference on Electrical Machines and Systems), Seoul, Korea, pp. 62–67, 2010.
- [17] Okedu, K.E. Muyeen, S.M. Takahashi, R. Tamura, J., "Stabilization of wind farms by DFIG-based variable speed wind generators," In Proceedings of the International Conference of Electrical Machines and Systems (ICEMS), Seoul, Korea, pp. 464–469, 2010.
- [18] Bekakra, Y. Attous, D.B., "Sliding Mode Controls of Active and Reactive Power of a DFIG with MPPT for Variable Speed Wind Energy Conversion," *Australian Journal Basic Applied Science.*, vol. 5, pp.2274–2286, 2011.
- [19] Ali, D.M. Jemli, K. Jemli, M. Gossa, M., "Doubly Fed Induction Generator, with Crowbar System under Micro-Interruptions Fault," *Int. J. Electr. Eng. Inform.*, vol. 2, pp. 216–231, 2010.
- [20] Suthar, D.B., "Wind Energy Integration for DFIG Based Wind Turbine Fault Ride Through," *Indian Journal Appl. Res.* vol. 4, pp, 216–220, 2014.
- [21] Lamchich, M.T. Lachguer, N., "Matlab, Simulink as Simulation Tool for Wind Generation Systems Based on Doubly Fed Induction Machines," In MATLAB—A Fundamental Tool for Scientific Computing and Engineering Applications Chapter 7 INTECH Publishing: Horwich, UK, vol. 2, pp. 139–160, 2012.
- [22] Noubrik, A. Chrifi-Alaoui, L. Bussy, P. Benchaib, A., "Analysis and Simulation of a 1.5MVA Doubly Fed Wind Power in Matlab Sim PowerSystems using Crowbar during Power Systems Disturbances," In Proceedings of the IEEE-2011 International Conference on Communications, Computing and Control Applications (CCCA), Hammamet, Tunisia, pp. 3–5, March 2011.
- [23] Nasiri, M. Mohammadi, R., "Peak current limitation for grid-side inverter by limited active power in PMSG-based wind turbines during different grid faults," *IEEE Transaction Sustain. Energy*, vol. 8, pp. 3–12, 2018.
- [24] Gencer, A., "Analysis and control of fault ride through capability improvement PMSG based on WECS using active crowbar system during different fault conditions," *Elektron. Elektrotech*, vol. 24, pp.64–69, 2018.
- [25] Yehia, D.M. Mansour, D.A. Yuan, W., "Fault ride-through enhancement of PMSG wind turbines with DC microgrids using resistive-type SFCL," *IEEE Transaction Applied Supercond.* vol. 28, pp,1–5, 2018.
- [26] M. Ragab, H. A. Abdushkour, A. F. Nahhas and W. H. Aljedaibi, "Deer hunting optimization with deep learning model for lung cancer classification," *Computers, Materials & Continua*, vol. 73, no.1, pp. 533–546, 2022.
- [27] X. R. Zhang, W. F. Zhang, W. Sun, X. M. Sun and S. K. Jha, "A robust 3-D medical watermarking based on wavelet transform for data protection," *Computer Systems Science & Engineering*, vol. 41, no. 3, pp. 1043–1056, 2022.
- [28] Y. Y. Ghadi, I. Akhter, S. A. Alsuhibany, T. A. Shloul, A. Jalal, *et al.*, "Multiple events detection using context-intelligence features," *Intelligent Automation & Soft Computing*, vol. 34, no.3, pp. 1455–1471, 2022.

#### **Contribution of Individual Authors to the Creation of a Scientific Article (Ghostwriting Policy)**

The authors equally contributed in the present research, at all stages from the formulation of the problem to the final findings and solution.

#### **Sources of Funding for Research Presented in a Scientific Article or Scientific Article Itself**

No funding was received for conducting this study.

#### **Conflict of Interest**

The authors have no conflicts of interest to declare that are relevant to the content of this article.

#### **Creative Commons Attribution License 4.0 (Attribution 4.0 International, CC BY 4.0)**

This article is published under the terms of the Creative Commons Attribution License 4.0

[https://creativecommons.org/licenses/by/4.0/deed.en\\_US](https://creativecommons.org/licenses/by/4.0/deed.en_US)